

## Hybrid Improper Ferroelectricity: A Mechanism for Controllable Polarization-Magnetization Coupling

Nicole A. Benedek and Craig J. Fennie

*School of Applied and Engineering Physics, Cornell University, Ithaca, New York 14853 USA*

(Received 11 December 2010; published 7 March 2011)

First-principles calculations are presented for the layered perovskite  $\text{Ca}_3\text{Mn}_2\text{O}_7$ . The results reveal a rich set of coupled structural, magnetic, and polar domains in which oxygen octahedron rotations induce ferroelectricity, magnetoelectricity, and weak ferromagnetism. The key point is that the rotation distortion is a combination of two nonpolar modes with different symmetries. We use the term “hybrid” improper ferroelectricity to describe this phenomenon and discuss how control over magnetism is achieved through these functional antiferrodistortive octahedron rotations.

DOI: 10.1103/PhysRevLett.106.107204

PACS numbers: 75.85.+t, 77.80.Fm, 81.05.Zx

The utility of multiferroics for low-power electronic devices stems from the possibility for electric-field control of magnetism at room temperature [1,2]. It has so far not been possible to identify a stable, single-phase multiferroic material in which the magnetization can be deterministically switched  $180^\circ$ . A large electrical polarization strongly coupled to the magnetization is generally thought to be a key requirement [3].

Magnetically driven improper ferroelectrics, such as  $\text{TbMnO}_3$ , are materials in which a spontaneous polarization arises due to symmetry-breaking by a spin instability [4]. These materials naturally have a strong coupling between magnetism and the polarization, but the polarization is too small for device applications. In known multiferroic materials with a large electrical polarization, such as  $\text{BiFeO}_3$  [5], the ferroelectricity is proper, originating from a zone-center polar lattice instability, as in the prototypical perovskite ferroelectric  $\text{PbTiO}_3$ . However, except in a few special cases that satisfy restrictive symmetry criteria, the polar instability in a proper ferroelectric does not break the right symmetries to turn on a nonzero magnetization and therefore does not satisfy the criteria of the only known mechanism that enables the electric field switching of the magnetization [6].

It is desirable to identify a more general mechanism—applicable to a large class of materials, for example, the  $\text{ABO}_3$  perovskites—whereby ferroelectricity and ferromagnetism are induced by the same lattice instability. Octahedron rotations, ubiquitous in perovskites and related materials, are natural candidates for this lattice instability as they are known to strongly couple to magnetic properties [7–9]. Unfortunately, such distortions (or combinations of distortions) in simple perovskites are not polar and therefore do not induce ferroelectricity. Recently, however, Bousquet, *et al.* [10] made a key discovery that by layering perovskites in an artificial superlattice, e.g.,  $(\text{SrTiO}_3)/(\text{PbTiO}_3)$ , a polarization can arise from the coupling of two rotational modes. Taking advantage of this mechanism to realize a strongly coupled multiferroic is a challenge.

In this Letter, we demonstrate how octahedron rotations simultaneously induce ferroelectricity, magnetoelectricity, and weak ferromagnetism in a class of naturally occurring  $(\text{ABO}_3)_2(\text{AO})$  layered perovskites. The key point is that the polarization,  $P$ , arises from a rotation pattern that is a combination of two nonpolar lattice modes with different symmetries,  $P \sim \mathcal{R}_1\mathcal{R}_2$ , as in Ref. [10], but here rotations  $\mathcal{R}_1$  and  $\mathcal{R}_2$  additionally induce magnetoelectricity and weak ferromagnetism respectively. We use the term “hybrid” improper ferroelectricity to describe this ferroelectric mechanism (in loose analogy to improper ferroelectricity [11] such as in  $\text{YMnO}_3$  [12]) in order to generalize the idea to include cases where the two distortion patterns do not necessarily condense at the same temperature. This mechanism has no impediment to room temperature operation and in fact opens up entirely new classes of materials in which to search for strongly coupled multiferroics. Our results show a rich set of coupled structural, magnetic, and polar domains and suggest the possibility to switch between magnetic domains with an electric field.

We have identified  $(\text{CaBO}_3)_2\text{CaO}$ , with  $B = \text{Ti}$  [13],  $\text{Mn}$  [14,15], as two materials that display hybrid improper ferroelectricity. It is significant that they occur in nature in bulk, forming in the Ruddlesden-Popper homologous family with general formula  $A_{n+1}B_n\text{O}_{3n+1}$ . Any given member of the Ruddlesden-Popper series consists of  $\text{ABO}_3$  perovskite blocks stacked along the [001] direction with an extra AO sheet inserted every  $n$  perovskite unit cells. For  $\text{Ca}_3\text{Mn}_2\text{O}_7$  ( $n = 2$ ) the experimental picture of the sequence of phase transitions from the paraelectric  $I4/mmm$  phase to the ferroelectric  $A2_1am$  phase is not clear. Two possibilities have been proposed: (1)  $I4/mmm \rightarrow Cmcm \rightarrow A2_1am$ , and (2) a direct transition from  $I4/mmm \rightarrow A2_1am$ . Additionally, it has been shown to display weak ferromagnetism [15,16]. To our knowledge,  $\text{Ca}_3\text{Ti}_2\text{O}_7$  has only been reported in the polar  $A2_1am$  structure. In the remainder of this Letter, we focus mainly on the magnetic compound,  $\text{Ca}_3\text{Mn}_2\text{O}_7$ , as a prototype of this class of strongly coupled multiferroics.

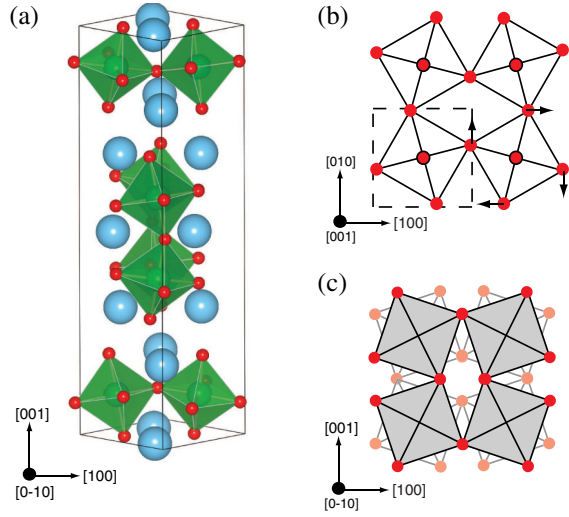


FIG. 1 (color online).  $\text{Ca}_3\text{Mn}_2\text{O}_7$  structure and rotation distortions. (a) The  $A2_1am$  ferroelectric ground state structure. Large (blue) spheres correspond to Ca ions. (b) Schematic of the atomic displacements corresponding to the  $X_2^+$  rotation. The dashed square denotes the unit cell of the  $I4/mmm$  parent structure. (c) Schematic of the  $X_3^-$  tilt mode. All axes refer to the coordinate system of the  $I4/mmm$  parent structure.

First-principles calculations were performed using density functional theory using projector augmented wave potentials within LSDA + U [17] as implemented in VASP [18,19]. All calculations were repeated within PBEsol + U, which provides an improved description of structural parameters; there was no qualitative change in any of our results. We used  $U = 4.5$  eV and  $J_H = 1$  eV for the Mn-ion on-site Coulomb and exchange parameters, respectively, common values for  $\text{Mn}^{4+}$  oxides (the results do not change for reasonable variations of  $U$ ). Where noted, noncollinear calculations with L-S coupling were performed. We used a 600 eV plane wave cutoff, a  $4 \times 4 \times 2$  Monkhorst-Pack mesh.

In the polar  $A2_1am$  structure, the oxygen octahedra are significantly rotated and tilted with respect to the  $I4/mmm$  structure, as shown in Fig. 1. The polarization, in the  $xy$  plane by symmetry, is found from our first-principles calculations to be large,  $P \approx 5 \mu\text{C}/\text{cm}^2$  ( $P \approx 20 \mu\text{C}/\text{cm}^2$  for  $\text{Ca}_3\text{Ti}_2\text{O}_7$ ). Group theoretical methods show that  $A2_1am$  is related to  $I4/mmm$  by three distinct atomic distortions: a polar zone-center mode transforming like the irreducible representation (irrep)  $\Gamma_5^-$ , and two zone-boundary modes at the  $X(1/2, 1/2, 0)$  point—an oxygen octahedron rotation mode with irrep  $X_2^+$  and an oxygen octahedron tilt mode with irrep  $X_3^-$ . Note that  $X_2^+ \oplus X_3^-$  establishes the  $A2_1am$  space group, a zone-center polar instability is not required. Hence, it is possible to reach the ferroelectric state by means of a combination of rotations and tilts only.

We project out the contribution of each  $X_3^-$ ,  $X_2^+$ , and  $\Gamma_5^-$  mode to the  $A2_1am$  ground state structure and calculate from first principles the  $T = 0$  energy surface around the

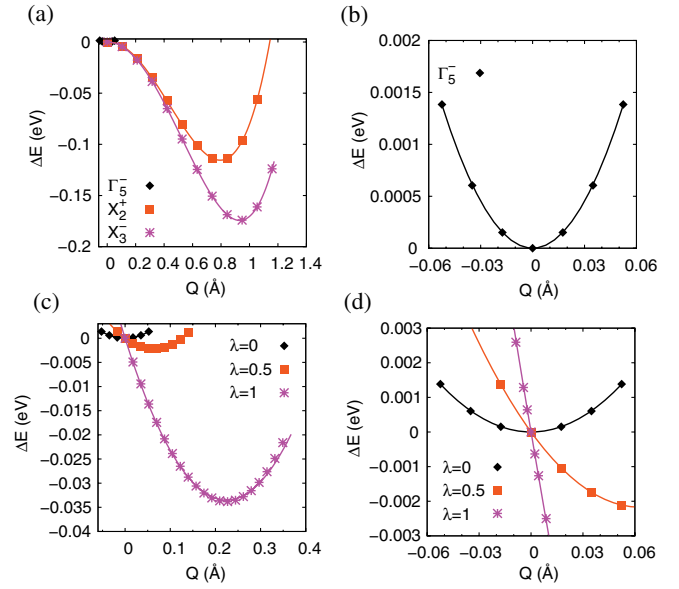


FIG. 2 (color online). Energy surface about paraelectric  $I4/mmm$  in  $\text{Ca}_3\text{Mn}_2\text{O}_7$ . Change in energy per formula unit as a function of the amplitude of (a), the  $X_2^+$  rotation and  $X_3^-$  tilt modes and (b), the polar  $\Gamma_5^-$  distortion. (c),(d) Polarization in the presence of a hybrid order parameter,  $Q_{X_{23}} = \lambda Q_{X_3^-} Q_{X_2^+}$ . Note the differences in scales between panels.

$I4/mmm$  reference structure. Figure 2(a) shows the total energy as a function of the amplitude of the distortion for the individual rotation ( $Q_{X_2^+}$ ), tilt ( $Q_{X_3^-}$ ), and polar ( $Q_{\Gamma_5^-}$ ) distortions. Relatively large energy gains can be seen within a characteristic double-well potential for the rotation and tilt distortions, whereas the polar contribution is stable, as shown in Fig. 2(b). Additionally, Fig. 3 shows that the combination of  $Q_{X_2^+}$  plus  $Q_{X_3^-}$  lowers the energy—even in the absence of the  $Q_{\Gamma_5^-}$  distortion—resulting in a ground state with four structural domains.

Figures 2(c) and 2(d) show how the polarization arises from a coupling to a hybrid order parameter  $Q_{X_{23}} = Q_{X_2^+} Q_{X_3^-}$ . In the absence of rotation and tilt distortions ( $Q_{X_{23}} = 0$ ), the polarization has a single minimum at  $P = 0$ . As  $Q_{X_{23}}$  increases, the polarization never becomes unstable. Rather, the minimum shifts to a nonzero value. The result of increasing  $Q_{X_{23}}$  is analogous to the effect of turning on a finite electric field, just like in the classic case of improper ferroelectricity [11]. Furthermore, when  $Q_{X_{23}} \neq 0$ , the polarization is linear about zero [Fig. 2(d)], a direct indication of improper coupling

$$\mathcal{F} = \alpha P Q_{X_2^+} Q_{X_3^-}$$

between the polarization, rotations, and tilts.

These observations suggest that the rotation mode and the tilt mode are the primary modes driving the transition to the ferroelectric  $A2_1am$  phase. This single distortion pattern,  $Q_{X_{23}}$ , is the hybrid improper mode. In contrast to proper and conventional improper ferroelectrics, more than

one lattice distortion may switch the polarization in a hybrid improper ferroelectric. Symmetry implies, and our calculations confirm, that the polarization reverses by either switching a  $X_2^+$  distortion or a  $X_3^-$  distortion but not both, resulting in two polar domains.

As is often the case in perovskites and related materials, octahedron rotations directly couple to the magnetic ordering. We determined from first principles the magnetic ground state of  $A2_1am$   $\text{Ca}_3\text{Mn}_2\text{O}_7$  with polarization along [010] to be antiferromagnetic ( $G$ -type within the perovskite bilayer). The spins point along [001] due to crystal-line anisotropy. Additional spin-orbit interactions give rise to a net spin-canted moment of  $M \approx 0.18\mu_B$  per unit cell (4 spins) along [100]. These results are consistent with previous experiments. Note that the magnetic point group,  $2'mm'$ , allows for a linear magnetoelectric effect [3], which symmetry indicates is induced by the  $X_2^+$  rotation distortion. Application of Dzyaloshinskii's criteria [20,21] shows the canted moment is the result of the  $X_3^-$  tilt distortion. Indeed, if we compute the magnetic ordering in the  $Cmcm$  ( $Cmca$ ) structure obtained by freezing in the  $X_3^-$  ( $X_2^+$ ) mode alone, we find  $M \approx 0.22\mu_B$  ( $M = 0\mu_B$ )

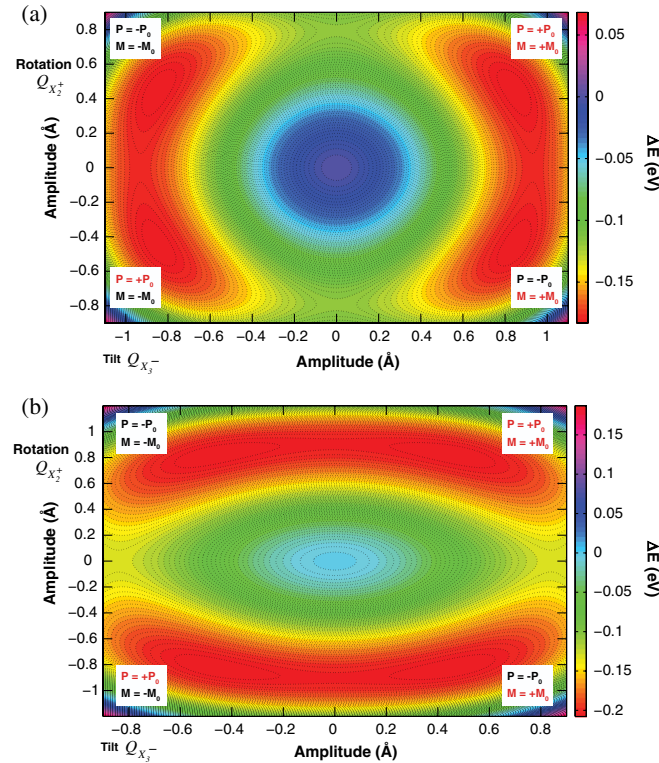


FIG. 3 (color online). Four types of structural domains and possible paths for electric-field switching of the magnetization in  $\text{Ca}_3\text{Mn}_2\text{O}_7$ . (a) Unstrained (bulk): Starting from a fixed  $X_3^-$  tilt domain, switch polarization by switching  $X_2^+$  rotation:  $P_0 \rightarrow -P_0$  and  $M_0 \rightarrow M_0$ . (b) Compressive biaxial strain: Start from a fixed  $X_2^+$  rotation domain, switch polarization by switching  $X_3^-$  tilts:  $P_0 \rightarrow -P_0$  and  $M_0 \rightarrow -M_0$ . The energy change is per formula unit.

per unit cell, which reverses with reversal of this octahedral tilt [22] resulting in two magnetic domains.

So which distortion, the rotation or the tilt, reverses in an electric-field switching experiment? Although polarization switching in a ferroelectric is a complex, dynamic process, we may gain some insight by examining the intrinsic energy barriers between domains. As shown in Fig. 3(a), the lowest energy pathway to switch the direction of the polarization is along the  $X_2^+$  switching path. In this process the magnetization does not reverse its sign. The linear magnetoelectric effect, however, is induced by the  $X_2^+$  distortion as mentioned. This electric-field tunable oxygen rotation distortion may lead to an enhanced magnetoelectric effect. Such calculations are beyond the scope of this Letter, but future theoretical and experimental studies should make this clear.

Oxygen rotations in perovskites are known to respond strongly to pressure and epitaxial strain. Figure 3(b) shows the energy landscape around the  $I4/mmm$  paraelectric structure at 1.5% compressive strain. Now the lowest energy pathway to switch the polarization to a symmetry equivalent state is along the  $X_3^-$  switching path, which as previously discussed, switches the direction of the spin-canted moment. Therefore, for an epitaxial thin film compressively strained in the  $A2_1am$  phase, we predict that switching the direction of the polarization with an electric field will switch the direction of the equilibrium magnetization by  $180^\circ$ . As in all experiments to date based on the linear magnetoelectric effect, however, a single antiferromagnetic domain must be annealed and maintained throughout the experiment.

This observation of tuning the intrinsic energy barriers between the domains with strain can be understood from well-known simple physical considerations [23]. Figure 4 shows the behavior of the rotation and tilt distortions in  $\text{Ca}_3\text{Mn}_2\text{O}_7$  under 1.5% biaxial tensile and compressive strains. Figure 4(a) shows that the energy lowering of the  $X_2^+$  rotation is strongly reduced under tensile strain compared with the unstrained state shown in Fig. 2(a). Under compressive strain, the opposite behavior occurs: the  $X_2^+$  mode is strongly favored, lowering the energy even more

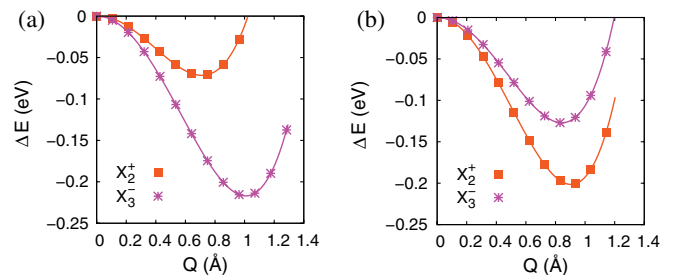


FIG. 4 (color online). Effect of epitaxial strain on the unstable zone-boundary modes in  $\text{Ca}_3\text{Mn}_2\text{O}_7$ . Change in energy per formula unit with regard to paraelectric  $I4/mmm$ , as a function of the amplitudes of the  $X_3^-$  and  $X_2^+$  modes under (a) 1.5% tensile and (b) 1.5% compressive biaxial strain. The lines are a guide to the eye (similar results were also found for  $\text{Ca}_3\text{Ti}_2\text{O}_7$ ).

than the  $X_3^-$  tilt mode, as shown in Fig. 4(b). We emphasize that strain does not induce, enhance, or mediate the polarization-magnetization coupling responsible for the electric-field switching of the magnetization in these materials. In the specific case of  $\text{Ca}_3\text{Mn}_2\text{O}_7$ , strain merely alters the energy landscape around the  $I4/mmm$  paraelectric structure, biasing one hybrid improper ferroelectric switching pathway (the one that simultaneously switches the direction of the magnetization) over the other. However, there is no fundamental reason why electric-field switching of the magnetization cannot be observed in bulk hybrid improper ferroelectrics.

In addition to the measurements already suggested, spatially resolving the structural, polar, and magnetic domains, e.g., optically [24], should prove the coupling physics discussed even in bulk  $\text{Ca}_3\text{Mn}_2\text{O}_7$ . It would also be of interest to understand the phase transition sequence from the high-symmetry paraelectric  $I4/mmm$  phase to the low-symmetry ferroelectric  $A2_1am$  phase. In bulk, two possibilities have been proposed as we previously discussed [25]. Path (1), having an intermediate  $Cmcm$  phase, is consistent with Landau theory and with our calculated hierarchy of structural distortions as displayed in Fig. 3(a). If Path (2) turns out to be correct, however, this indicates that the two distortions making up the hybrid order parameter condense at the same temperature, analogous to the recent discovery of Ref. [10]. Regardless of the actual path taken—or even if a paraelectric structure is realizable in the phase diagram of the system—our conclusions on the coupling of rotation or tilt distortions to ferroelectricity and magnetism remain unchanged.

Note that the temperature scale of the hybrid improper ferroelectric mechanism is set by the structural distortions, which commonly occur above room temperature ( $\sim 500\text{--}600$  K in  $\text{Ca}_3\text{Mn}_2\text{O}_7$  [26]). The “limiting” temperature in the case of  $\text{Ca}_3\text{Mn}_2\text{O}_7$  is the Néel temperature,  $T_N \sim 115$  K [15,16] and as such this prototype material is not ideal. There is, however, no fundamental reason why one could not discover (or design) a hybrid improper ferroelectric with a Néel temperature above room temperature (ongoing investigations have realized initial materials design rules [27]), so the mechanism has no impediment to room-temperature operation. This approach therefore shifts the challenge of discovering a multiferroic in which the magnetization can be controlled by the electrical polarization to the more familiar problem of designing a room-temperature antiferromagnet.

In summary, we have introduced the term hybrid improper ferroelectricity to describe a state in which the polarization is *induced* by a complex distortion pattern consisting of more than one octahedron rotation mode. We have shown how this mechanism opens up new avenues to pursue strong polarization-magnetization coupling, as alluded to in Ref. [10] and realized in this Letter, and discovered a new class of materials. We hope our Letter inspires further work in this intriguing field of materials with functional rotations and tilt distortions.

We acknowledge discussions with V. Gopalan, D. G. Schlom, K. M. Rabe, and M. Stengel. N. A. B. was supported by the Cornell Center for Materials Research with funding from NSF MRSEC program, cooperative Agreement No. DMR 0520404. C. J. F. was supported by the DOE-BES under Grant No. DE-SC0002334.

- 
- [1] Y. Tokunaga, N. Furukawa, H. Sakai, Y. Taguchi, T.-h. Arima, and Y. Tokura, *Nature Mater.* **8**, 558 (2009).
  - [2] M. Bibes and A. Barthelemy, *Nature Mater.* **7**, 425 (2008).
  - [3] W. Erenstein, N. D. Mathur, and J. F. Scott, *Nature (London)* **442**, 759 (2006).
  - [4] T. Kimura, T. Goto, H. Shintani, K. Ishizaka, T. Arima, and Y. Tokura, *Nature (London)* **426**, 55 (2003).
  - [5] J. Wang, J. B. Neaton, H. Zheng, V. Nagarajan, S. B. Ogale, B. Liu, D. Viehland, V. Vaithyanathan, D. G. Schlom, U. V. Waghmare *et al.*, *Science* **299**, 1719 (2003).
  - [6] C. J. Fennie, *Phys. Rev. Lett.* **100**, 167203 (2008).
  - [7] A. J. Millis, *Nature (London)* **392**, 147 (1998).
  - [8] T. Goto, T. Kimura, G. Lawes, A. P. Ramirez, and Y. Tokura, *Phys. Rev. Lett.* **92**, 257201 (2004).
  - [9] M. Rini, R. Tobey, N. Dean, J. Itatani, Y. Tomioka, Y. Tokura, R. W. Schoenlein, and A. Cavalleri, *Nature (London)* **449**, 72 (2007).
  - [10] E. Bousquet, M. Dawber, N. Stucki, C. Lichtensteiger, P. Hermet, S. Gariglio, J.-M. Triscone, and Ph. Ghosez, *Nature (London)* **452**, 732 (2008).
  - [11] A. P. Levanyuk and D. G. Sannikov, *Usp. Fiz. Nauk* **112**, 561 (1974).
  - [12] C. J. Fennie and K. M. Rabe, *Phys. Rev. B* **72**, 100103 (2005).
  - [13] M. M. Elcombe, E. H. Kisi, K. D. Hawkins, T. J. White, P. Goodman, and S. Matheson, *Acta Crystallogr. Sect. B* **47**, 305 (1991).
  - [14] N. Guiblin, D. Grebille, H. Leligny, and C. Martin, *Acta Crystallogr. Sect. C* **58**, i3 (2001).
  - [15] M. V. Lobanov, M. Greenblatt, E. N. Caspi, J. D. Jorgensen, D. V. Sheptyakov, B. H. Toby, C. E. Botez, and P. W. Stephens, *J. Phys. Condens. Matter* **16**, 5339 (2004).
  - [16] W.-H. Jung, *J. Mater. Sci. Lett.* **19**, 2037 (2000).
  - [17] V. I. Anisimov, F. Aryasetiawan, and A. I. Lichtenstein, *J. Phys. Condens. Matter* **9**, 767 (1997).
  - [18] G. Kresse and J. Hafner, *Phys. Rev. B* **47**, 558 (1993).
  - [19] G. Kresse and D. Joubert, *Phys. Rev. B* **59**, 1758 (1999).
  - [20] I. Dzyaloshinskii, *J. Phys. Chem. Solids* **4**, 241 (1958).
  - [21] T. Moriya, *Phys. Rev.* **120**, 91 (1960).
  - [22] See supplementary material at <http://link.aps.org/supplemental/10.1103/PhysRevLett.106.107204>.
  - [23] G. A. Samara, T. Sakudo, and K. Yoshimitsu, *Phys. Rev. Lett.* **35**, 1767 (1975).
  - [24] B. B. Van Aken, J.-P. Rivera, H. Schmid, and M. Fiebig, *Nature (London)* **449**, 702 (2007).
  - [25] In compressively strained films an alternative path, Fig. 3(b), would be  $I4/mmm \rightarrow Cmca \rightarrow A2_1am$ .
  - [26] L. Bendersky, M. Greenblatt, and R. Chen, *J. Solid State Chem.* **174**, 418 (2003).
  - [27] J. M. Rondinelli and C. J. Fennie (to published).